Impact of Fouling on Flow-induced Vibration Characteristics in Fluid-conveying Pipelines

JIANFENG HUANG[1,2], *Member, IEEE*, GUOHUA CHEN[1], LEI SHU[2], *Senior Member, IEEE*, YUANFANG CHEN[2], *Member, IEEE* , AND YU ZHANG[3]
[1] Institute of Safety Science and Engineering, South China University of Technology, Guangzhou 510640, China
[2] Guangdong Petrochemical Equipment Fault Diagnosis Key Laboratory, Guangdong University of Petrochemical Technology, Maoming 525000, China
[3] School of Engineering, University of Lincoln, Lincoln LN6 7TS, U.K
Corresponding authors: G. Chen (mmghchen@scut.edu.cn) and L. Shu (lei.shu@ieee.org)

***Abstract*—This paper addresses monitoring problems commonly encountered in petrochemical enterprises caused by fouling and clogging in the circulating water heat exchangers by monitoring the heat exchanger's wall vibration signal for early failure detection. Due to the difficulties encountered in simulation caused by the large number of tubes inside the heat exchanger, such methods were discussed by studying in the fluid-conveying pipeline fouling. ANSYS was used to establish the normal model and fouling model of a fluid-conveying pipeline so as to analyze the changing rule of various parameters that are influenced by different inlet velocities. As the inlet velocity and fouling severity continuously increased, the wall load and the vibration acceleration increased as well, leading variations in wall vibration signals. This paper conduct extensive experiments by using straight pipes to compare the results from simulation and from normal fluid-conveying pipelines, under the same working conditions. By such comparison, we estimate the accuracy of the simulation model.**

***Index Terms*—Fluid-conveying pipelines, fouling impact, vibration characteristics, vibration signals.**

I. INTRODUCTION

THE circulating water heat exchanger is used universally to exchange heat, in modern petrochemical enterprises, and accounts for 40% of the overall investment in facilities. The maintenance workload accounts for approximately 60–70% of the total maintenance workload. The safe operation of a heat exchanger is of great significance to continuous production of these enterprises. The fluid movement within the shell-and-tube heat exchanger is extremely complex, and includes transverse flow, axial flow, bypass flow, etc. There is a stagnant zone at both ends of the bundles, where flow velocity and direction changes are irregular. The heat transfer tubes are in a non-uniform force field under the influence of various excitation forces caused by fluid flow, which easily generates vibrations [1]. The forming of deposits and fouling are very likely when industrial circulation water, the cooling medium of a heat exchanger, is used. Appropriate vibration is beneficial in helping to reduce fouling, and serious fouling lowers the heat exchange efficiency. To maintain its original efficiency, accelerating the velocity is required, which leads to increased heat exchanger vibration. According to statistics, approximately 30% of damage to heat exchangers is caused by bundle vibration[2]. Therefore, the study of vibrations related to circulation water heat exchanger fouling and clogging is of realistic significance.

At present, some researchers have carried out simulation studies on optimizing the heat exchange tube structure, heat exchange performance, and parameters of the heat changer by means of ANSYS [3-5]. However, there are few achievements on the malfunctioning vibration characteristics of the heat exchanger through commercial simulation software, because fluidic and structural two-way coupling is involved, and the heat exchanger is extremely large, leading to difficulties in the analysis and calculation of a finite element. Hence, this paper describes studies conducted on fluid-conveying pipeline fouling and vibration to identify methods that can be used to diagnose heat exchanger malfunctions caused by vibration signals.

The heat transfer tube is one of the basic components of a circulating water heat exchanger used to transfer and control liquid or gas. The number of heat transfer tubes located inside the heat exchanger varies from several to thousands. The bundles of the shell-and-tube circulating water heat exchanger are normally straight, and the heat transfer tubes are considered a combination of various types of beams. Normally, the pipeline between two baffle plates is a simply supported single-span beam, and the pipeline between the tube plate and baffle plate is similarly a single-span beam with one fixed end and one simply supported end [6]. Therefore, further study of the vibration characteristics of heat transfer tube fouling of heat exchangers through the vibration characteristic analysis of fluid-conveying-fouling pipeline is proposed.

The contributions of this paper are listed as follows:

This work is supported by National Natural Science Foundation of China (NO.61401107 and NO. 21576102), International and Hong Kong, Macao & Taiwan collaborative innovation platform and major international cooperation projects of colleges in Guangdong Province (No.2015KGJHZ026), The Natural Science Foundation of Guangdong Province (No.2016A030307029), the Open Fund of Maoming Study and Development Center of Petrochemical Corrosion and Safety Engineering (No.201509A01), the Open Fund of Guangdong Provincial Key Laboratory of Petrochemical Equipment Fault Diagnosis (No.GDUPTLAB201605), Guangdong University of Petrochemical Technology through Internal Project 2012RC106.

1) The bundles of circulating water heat exchanger were divided into numerous fluid-conveying pipelines. Heat exchanger pipeline fouling was studied and discussed, resulting in a new diagnostic method.
2) A finite element model was put forward to analyze the fluid-conveying pipeline fouling. By studying the models' different fouling levels, this paper determined the pattern of pipeline vibration caused by pipeline fouling.
3) The vibration test experiments were conducted on a non-fouling, fluid-conveying pipeline, which proved the correctness of the pipeline finite element model.

The remainder of this paper was organized as follows. The related work about pipeline fouling and pipeline vibration was briefly introduced in Section II. Section III described the pipeline cell stress analysis and section IV presented the basic simulation theories. The pipeline simulation model were built in section V and section VI. The experimental analysis of normal pipelines was given in Section VII. Finally, Section VIII presented the overall conclusions.

II. RELATED WORK

Because fluid-conveying pipeline vibration accelerates fatigue damage, shortens the lifespan of, and causes harm to materials (e.g., the connector crack), scholars have carried out extensive research on pipeline vibration.

Silva [7-8] presented preliminary research results of vibrational hammer excitation for easy to use external non-invasive, non-destructive fouling detection in pipelines. The proposed method could detect the inner pipe layer formation, and thickness estimation of the adsorbed material. Then, Silva [9-11] analyzed the vibration signals in presence of an inner pipe fouling layer using an accelerometer and a microphone for detection. The paper outlined the experimental setup, achievable sensitivities and limitations of the method. Carellan [12] presented a critical review of the state of the art of the approaches based on ultrasonic vibration of the pipe. This paper also analyzed the limitations that were pertinent to the prevention of fouling in pipes. Ren[13] analyzed the vibration induced from fluid-structure interaction in liquid-filled pipes using the traveling wave method. The vibration characters in two types of coupled problems such as the junction interaction in liquid-filled pipes and the pipe vibration stability are analyzed. The thin wall cylindrical tube with both fixed support ends was simplified to a beam model by Li [14] and other scholars. In addition, the flexural vibration beam theory, together with finite element methods, was adopted in producing a natural frequency and vibration type of cylindrical tube, around which experiments were designed. By comparing the theoretical value with the experimental value, was discovered that the fluid causes the decline of the natural frequency of cylindrical tube.

Guo [15] established a finite element model of a straight fluid conveying pipe by ANSYS. The dynamic responses of the pipeline with a given input fluid flow velocities pulse, in three different supported modes, were simulated using the finite element method and the method of computational fluid dynamics. The results of pipe vibration, including the displacement of pipe wall points, fixed pivot reacting force, cross-sectional displacement and stress, were analyzed. ANSYS simulation technology was used by Li [16] to study the impact of fluid-solid coupling on fluid-filled pipeline vibration modality and the impact of variation constraint on fluid-filled pipeline forces as well as its vibration modality. It was discovered that the fluid-solid coupling and increased constraint variation resulted in a rise in pipeline vibration frequency and a significant decline in pipeline equivalent stress and total deflection. Wu [17] and other scholars used a finite element method to conduct modal analysis and harmonic response analysis on high pressure pipe. In the meantime, the impact on pipeline vibration frequency caused by increased clamp support and location changes were analyzed. This led to the conclusion that the presence of prestress would increase the pipeline's natural vibration frequency. Wang [18] used fluid-filled pipe for flow field simulation and discovered the pressure changing characteristics of the pipe with the periodic initial velocities. They further combined with the one-way coupling module of an ANSYS workbench, and obtained the fluid-solid coupling vibration modal characteristics of fluid-filled pipe under the influence of fluctuating pressure and the impact of pipeline support distance on vibration modal.

Wu [19] presented a simplified model for the numerical simulation of blockage pipe detection based on the principle of auto-oscillation theory. The result shown that the blockage damping was direct ratio to the flow velocities of pipe and the location of damping had the cosine relation with damping parameters so the location and magnitude of blockage could be fixed if two blockage damping parameters were known. Zhu [20] put forward the basic continuity equation which could be used to calculate the coupled water hammer based on the existing theory of water hammer and its coupled theory. Chen [21] presented an experimental method of non-contact vibration measurement to study the parametric resonance of a pipe conveying fluid. The result showed that at a certain flow velocity, the phenomena of parametric resonance could occur with the proper pulsating amplitude and frequency and the position of parametric resonance regions were closely related to flow velocity. Qi [22] built a model of fluid conveying pipe using finite element pack ANSYS and hydrokinetics pack CFX. The data was exchanged between two packs for fluid –solid coupling analysis. The vibration characteristic of the pipe impacting in a ramp increase velocity was analyzed. The vibration respondence of the pipe was calculated in a half sine wave excitation.

The above research mainly analyzed the vibration characteristics of fluid-conveying pipeline without taking the malfunction caused by pipeline fouling into consideration. The fouling pipelines in exchangers would lead to clogging fault. Huang [23] proposed a new fault diagnose method based on vibration signals and support vector machine. An experimental model of clogging fault diagnosis in heat exchangers was studied. The experimental results have shown that the proposed method was efficient and had achieved a high accuracy for benchmarking vibration signals under both normal and faulty conditions. This paper primarily describes the study of the

influences on vibration caused by fouling in fluid-conveying pipelines.

III. CELL STRESS ANALYSIS

There are many causes behind vibration in fluid-conveying pipeline. The three main reasons are as follows [18, 24]: (1) It was caused by the poor dynamic balance of the power machines or inappropriate base installation; (2) The vibration was caused by pulsating flow; (3) The vibration was caused by the fluid vortex and air column resonance inside the pipeline. Engineering practices show that, when flexible connection pipes were installed or damping measures were used, the pipeline vibration was primarily caused by pulsating flow [25]. The initiating terminal facilities of power machines, such as a centrifugal pump moved in periodic intermittent motion, led to changes in parameters such as pressure, velocity, density, and flow in the pipeline with variations of time and position. Thus, pulsating flow was generated. Below we primarily analyze the forces of fluid-conveying pipeline from the perspective of the impact of pulsating flow.

When unsteady liquid was transported, pulsating flow caused pipeline vibration [6]. An assumption was made that the pipeline vibrated slightly within the elastic range because of pulsating flow. As shown in Fig.1, point A was randomly picked as the junction point of the fluid and the inside wall of a normal pipeline to conduct cell stress analysis, and the axial thrust of fluid at point A was set as F . Here, the main lateral force was pressure on the wall generated by pulsating flow, F_m.

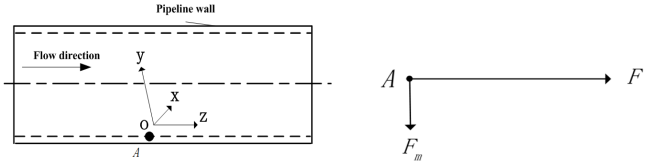

(A)The analyzed position (B)Stress analysis

Figure 1. The cell stress analysis of normal pipeline

The pressure F_m was the sum of an inertial force sharing the same acceleration as the flow and a drag force whose phase was the same as flow velocity.

A structure in accelerated motion was built in the accelerated flow[26], and its net inertial force at unit length was:

$$F_3 = \rho A \frac{\partial U}{\partial t} + C_1 \rho A \left(\frac{\partial U}{\partial t} - \frac{\partial^2 x}{\partial t^2} \right) \quad (1)$$

The drag force at structural unit length was:

$$F_E = \frac{1}{2} \rho C_E \left| U - \frac{\partial x}{\partial t} \right| \left(U - \frac{\partial x}{\partial t} \right) D_1 \quad (2)$$

In this equation, ρ is set as the fluid density, A is the structural cross section (m^2), C_1 is the added mass coefficient, U is the mean velocity of transient flowing fluid cross section (m/s), C_E is the drag force coefficient, and D_1 as the width of the structure approaching the flow section. In addition, the direction of drag force was consistent with the direction of the relative velocity of both fluid and structure $\left(U - \frac{\partial x}{\partial t} \right)$.

Therefore, the resultant force was:

$$F_m = F_3 + F_E = \rho A \frac{\partial U}{\partial t} + C_1 \rho A \left(\frac{\partial U}{\partial t} - \frac{\partial^2 x}{\partial t^2} \right) + \frac{1}{2} \rho C_E \left| U - \frac{\partial x}{\partial t} \right| \left(U - \frac{\partial x}{\partial t} \right) D_1 \quad (3)$$

When the fluctuation velocity surpassed vibration velocity to a large extent, $\left| U - \frac{\partial x}{\partial t} \right| \left(U - \frac{\partial x}{\partial t} \right)$ could be simplified as $|U|U$, and equation (3) could be simplified as:

$$F_m = \rho (1 + C_1) \ A \frac{\partial U}{\partial t} + \frac{1}{2} \rho C_E |U| U D_1 \quad (4)$$

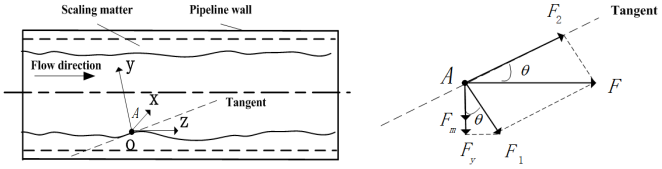

(A)The analyzed position (B)Stress analysis

Figure 2. The cell stress analysis of fouling pipeline

The inner wall of pipeline would be covered in a thick layer of stemming after fouling. As shown in Figure 2, point A was randomly picked from the interface of fluid and stemming for stress analysis, and the included angle of F and wall tangent was set as θ. In the meantime, F could be divided into two forces: F_1 in the normal direction, and F_2 in the tangential direction. Likewise, F_1 was decomposed into the axial component and the lateral component F_y. The following result was obtained through the triangle::

$$F_1 = F \sin\theta \quad (5)$$

$$F_2 = F \cos\theta \quad (6)$$

$$F_y = F_1 \cos\theta = F \sin\theta \cos\theta \quad (7)$$

At this point, the lateral force was $F_m + F_y$, which indicated an increase in the fouling pipeline's lateral, which is one of the reasons it vibrated more violently than the normal pipeline.

IV. SIMULATION THEORY

The ANSYS-CFX solution method was used in this paper to conduct simulation research on a fluid-conveying pipeline. To obtain the changing status of vibration acceleration, a two-way coupling separation solution was adopted. For starters, this study used a flow field analysis module to calculate the flow field of a fluid-conveying pipeline. Afterward, a structural dynamics analysis using a structural analysis module was used to calculate surface pressure results and surface velocity results. The structural distortion was transferred to CFX to conduct flow field analysis. Such an approach maximized the use of structural mechanics and fluid mechanics calculations. According to the given order, the solid control equation and fluid control equation was solved. In order to obtain more accurate simulation results, the results of solid and fluid control were transferred and exchanged through the contact surface.

In terms of fluid-solid coupling, seeking solutions to a structural dynamics equation, Navier-Stokes Equations, and a fluid continuity equation at the same time is required [27]:

The structural dynamics equation was:

$$[\mathrm{M}]\{\ddot{u}\} + [\mathrm{C}]\{\dot{u}\} + [\mathrm{K}]\{u\} = \{\mathrm{F}\} \quad (8)$$

In this equation, $[M]$ represented the overall structural mass matrix; $[K]$ represented the overall structural stiffness

matrix; [C] represented the overall structural damping matrix; [F] represented the structural load matrix, and {u} represented the structural displacement vector.

The fluid momentum equation was:

$$\frac{\partial \nu}{\partial t} + \nu(\nu \cdot \nabla) = -\frac{1}{\rho}\ (\nabla p + \mathrm{div}\tau) \qquad (9)$$

The fluid continuous equation was:

$$\frac{\partial \rho}{\partial t} + \nabla \cdot (\rho \nu) = 0 \qquad (10)$$

Where ∇ was Hamiltonian, t was time， p was fluid pressure, ρ was fluid density, ν was fluid velocity, τ was shearing force.

This paper did not take the energy equation into consideration, because energy transfer and conversion was not involved.

The turbulence model was used to conduct analysis on the simulation of flow field in the fluid-conveying pipeline. The standard k-ε model was adopted in the CFX [28], which was composed by the turbulent kinetic energy equation k and the diffusion equation ε.

The turbulent kinetic energy equation k *was*:

$$\frac{\partial(\rho k u_i)}{\partial x_i} = \frac{\partial}{\partial x_j}\left[\left(\mu + \frac{\mu_t}{\sigma_k}\right)\frac{\partial k}{\partial x_j}\right] + P_k - \rho\varepsilon \qquad (11)$$

The diffusion equation ε was:

$$\frac{\partial(\rho \varepsilon u_i)}{\partial x_i} = \frac{\partial}{\partial x_j}\left[\left(\mu + \frac{\mu_t}{\sigma_\varepsilon}\right)\frac{\partial \varepsilon}{\partial x_j}\right] + \frac{\varepsilon}{k}(c_{\varepsilon 1}P_k - c_{\varepsilon 2}\rho\varepsilon) \qquad (12)$$

Where $k = \frac{1}{2}\overline{\mu_i' \mu_i'}$， $\varepsilon = \frac{\mu}{\rho}\left(\overline{\frac{\partial u_i}{\partial x_j}}\,\overline{\frac{\partial u_i}{\partial x_j}}\right)$

Turbulent viscosity μ_t expressed as function of k andε :

$$\mu_t = \rho c_\mu \frac{k^2}{\varepsilon} \qquad (13)$$

P_k represented the pressure-generating item caused by velocity gradient:

$$P_k = \mu_t\left(\frac{\partial u_i}{\partial x_j} + \frac{\partial u_j}{\partial x_i}\right)\frac{\partial u_i}{\partial x_j} \qquad (14)$$

Where $c_\mu = 0.09$， $c_{\varepsilon 1} = 1.44$， $c_{\varepsilon 2} = 1.92$, $\sigma_k = 1.0$， $\sigma_\varepsilon = 1.3$

The boundary condition of no-slip from integral to wall surface was $k = 0$ and $\varepsilon = 0$.

Starting from the turbulence model, the following portion of the study involved creating a normal fluid-conveying pipeline model without fouling by means of ANSYS to study the vibrations of pipeline under the influences of different flow velocities. Afterward, a fluid-conveying pipeline models were built with different fouling levels that were used to conduct research on the fouling pipeline vibrations with the premise of same flow velocity.

V. FINITE ELEMENT ANALYSIS ON NORMAL FLUID-CONVEYING PIPELINE

A. Model and Boundary Conditions

1) Basic model parameters

This paper established a finite element model of fluid-conveying pipeline and a finite model of fluid inside the pipeline. Galvanized steel pipeline was chosen, and specific parameters were as shown in Table I. In order to be consistent with the following experiments, the flow velocities at the entrance point of the fluid-conveying pipelines were set respectively as 0.33, 0.52, 0.74, and 1.01 m/s. Moreover, the mesh used in this model was divided into two parts: the structural mesh and the fluid domain mesh. The former was divided into 5,795 units and 35,158 nodes, while the latter was 43,946 units and 38,250 nodes.

TABLE I BASIC PARAMETERS OF PIPELINE MODEL

Item	Parameter	Item	Parameter
length	2000mm	yield strength	σ=0.25GPa
elasticity modulus	E =20GPa	Poisson's ratio	υ=0.3
density	7.85×10^3kg/m^3	environment temperature	25℃
fluid density （water）	ρ=1.0×10^3kg/m^3	pipe diameter	φ20×2mm

2) Boundary condition setting

First, the boundary condition of the structural body was set. The inner wall surface was set as the interface of fluid-solid coupling. In addition, the wall surface at both pipeline ends was set as the constraint condition of securing support, the gravity field was set as 9.8 m/s^2 with the direction of the −Y axis, and the inner wall surface was considered to be the loading surface of fluid pressure load.

Second, the boundary condition of the fluid domain was set. Transient analysis was adopted, because the bidirectional process was transient transfer, and the duration and step length analyzed should be the same as those in structural analysis. Dynamic mesh was chosen for the fluid domain, the heat transfer was shut down, and the k-epsilon turbulence model was used. The inlet flow velocities were set as fixed values. The pressure at exit points was set at 0 Pa, and the boundary of wall surface was considered to be the fluid-solid coupling surface. The total time length of solution was set as 1 s, the step length was set at 0.01 s, and appropriate condition of convergence was set in the CFX solver.

B. Pipeline Fluid Domain

The flow velocity nephogram of fluid domain was extracted to observe the flow velocity distribution and flow direction in the fluid-conveying pipeline. Figure 3, shows that in the pipeline model with different input flow velocities, the high flow velocity intensively distributed at the center of the pipeline when the fluid was running through. On the contrary, the flow velocity near the wall surface was low, and the flow velocities at the entry points were lower than those inside the pipeline. In addition, the direction of fluid was consistent, moving in toward the outlet in a rectilinear way. However, due to the uneven distribution of flow velocities inside the pipeline, there were velocity differences, which caused changes in pipeline load to a certain extent, which in turn generated pipeline vibration.

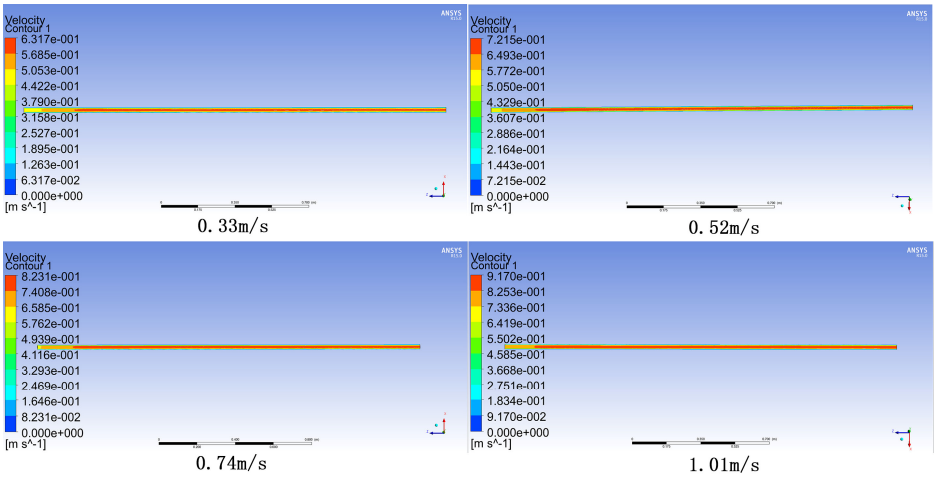

Figure 3. Flow velocity analysis of a pipeline

C. *Pipeline Wall Load*

As shown by the extracted pipeline wall load in Figure 4, the load showed a gradient decrement trend from inlet to outlet. The closer it was to the inlet, the larger the pipeline wall load became, while the closer it was to the outlet, the smaller the load became. With the continuous growth of inlet flow velocity, the wall load successively increased with the same load direction, radially covering the surface of pipeline wall. Combined with Figure 3, it was discovered that the load was relatively large at the wall of the inlet, while the inlet flow velocity was small. The differences in flow velocity at the inlet had a significant impact on the pipeline load, which increased with the growth of inlet flow velocity. According to the above analysis on the flow velocities inside the pipeline, it is apparent that the flow velocity differences in axial direction at the inlet are relatively large. Thus, it is concluded that flow velocity difference increase is one of the reasons for the larger load at the pipeline inlet.

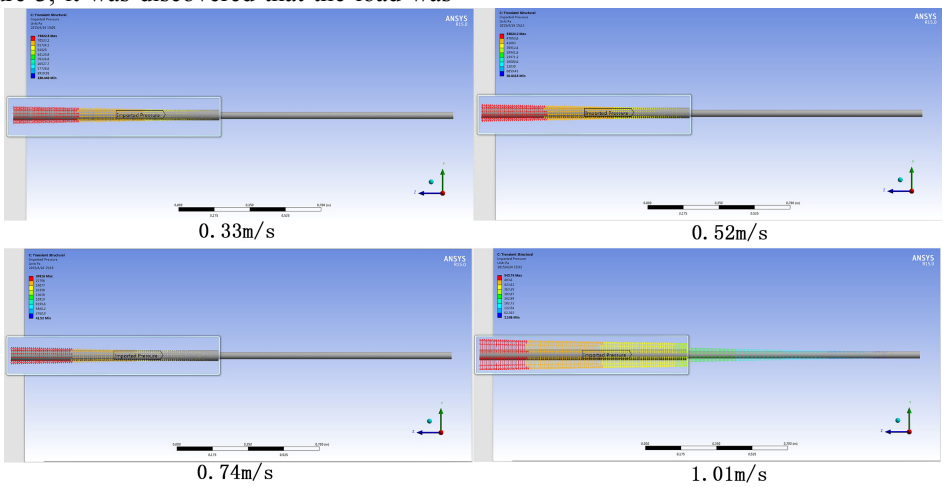

Figure 4. Wall load analysis of a pipeline

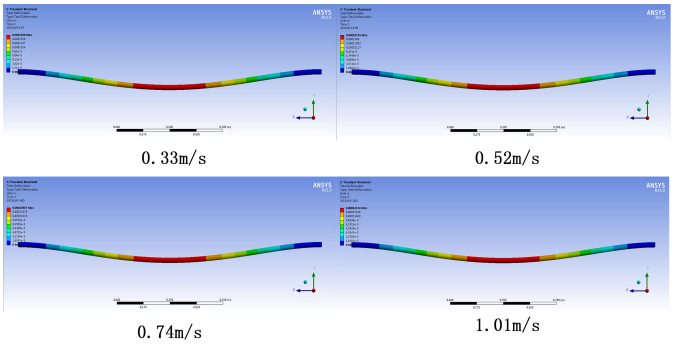

Figure 5. The displacement analysis of a pipeline

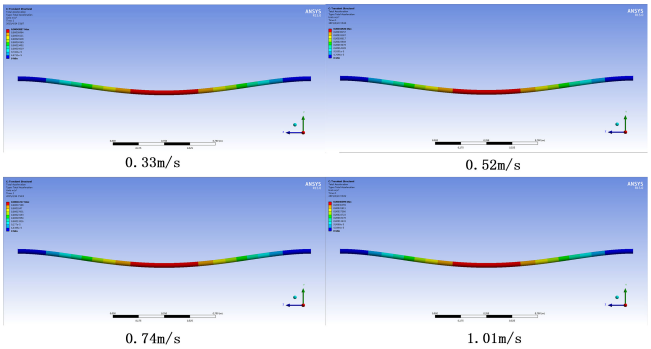

Figure 6. The acceleration analysis of a pipeline

D. *Wall Displacement and Acceleration*

The nephograms of pipeline wall displacement and acceleration were extracted as shown in Figures 5 and 6. With the five flow velocities in the computer model, the pipeline deformation was basically consistent. The relatively larger deformation appeared at the center of the pipeline, while the

relatively small deformation displacement symmetrically appeared at both ends of the pipeline, which was relevant to the constraints of pipeline model. Because the acceleration and displacement were quadratic integrals, the nephogram of wall displacement and acceleration nephogram showed a consistent changing trend.

Three positions, A (near inlet), B (near the center) and C (near outlet), were selected as the observation points on the same axis of the fluid-conveying pipeline. The average displacement values influenced by various flow velocities were as shown in table II. It was discovered that the average displacement values at these three observation points were different with different flow velocities. Flow velocity values are higher at the center and smaller at both ends. Moreover, displacement values increased consistently with the growth of flow velocity. Therefore, flow velocity is one of the main influences on vibration in fluid-conveying pipeline.

Three positions, A (near inlet), B (near the center) and C (near outlet), were selected as the observation points on the same axis of the fluid-conveying pipeline. The average

VI. FINITE ELEMENT ANALYSIS ON FOULING FLUID-CONVEYING PIPELINE

A. Model and Boundary Conditions

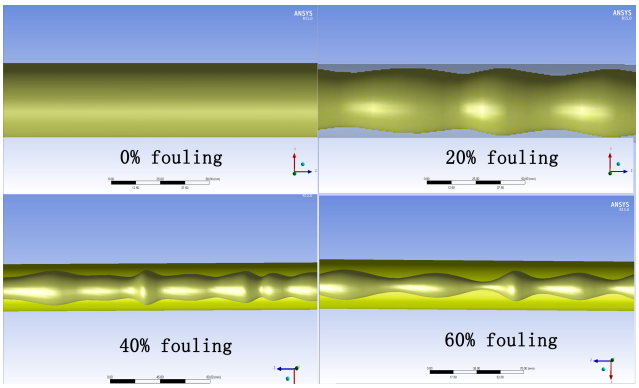

Figure 7. The side elevation of the fouling pipeline model

The basic parameters and boundary conditions of fouling fluid-conveying pipeline models were consistent with the above-mentioned fluid-conveying pipeline model under normal conditions. There were four levels of fouling: 0%, 20%, 40%, and 60% fouling. The stemming material was the same as that of the fluid-conveying pipeline. The percentages refer to the proportion of stemming inside the pipeline, and accounts for the whole volume of an empty pipeline. For the purposes of emphasizing the impact of fouling on vibration, the fouling levels were set at increments of 20%. As shown in the fouling model (Figure 7), the shapes of inner wall stemming were formed by rotating the random curve at 360°, and the flow velocity at the inlet was uniformly divided into two conditions: 0.4 m/s and 1.0 m/s.

B. Pipeline Fluid Domain

The flow velocities of fluid domain inside the fouling pipeline are shown in Figure 8. As opposed to the nephogram with evenly distributed flow velocities of fluid domain without fouling, the flow velocities of fluid domain inside the fouling pipeline changed with the stemming shape, and high flow velocities appeared in the positions where relatively intensive fouling exist. The distribution of the flow velocity of fluid domain inside the fouling pipeline was as follows: The positions near the pipeline wall distributed low flow velocity, while the center showed high flow velocity; at the locations where the stemming was heavily distributed, the direction of fluid changed suddenly, and the flow velocity increased drastically.

displacement values influenced by various flow velocities were as shown in table II. It was discovered that the average displacement values at these three observation points were different with different flow velocities. Flow velocity values are higher at the center and smaller at both ends. Moreover, displacement values increased consistently with the growth of flow velocity. Therefore, flow velocity is one of the main influences on vibration in fluid-conveying pipeline.

TABLE II THE AVERAGE DISPLACEMENTS OF EACH OBSERVATION POINT

Inlet flow velocity	Position A	Position B	Position C
0.23m/s	-0.6×10^{-6}m	-24.8×10^{-6}m	0.5×10^{-6}m
0.33m/s	-0.3×10^{-6}m	7.0×10^{-6}m	1.2×10^{-6}m
0.52m/s	0.3×10^{-6}m	70.9×10^{-6}m	2.5×10^{-6}m
0.74m/s	0.9×10^{-6}m	146.0×10^{-6}m	4.1×10^{-6}m
1.01m/s	1.8×10^{-6}m	238×10^{-6}m	6.0×10^{-6}m

C. Pipeline Wall Load Analysis

As shown in Figure 9, the distribution rules of wall surface load in the four conditions were consistent, which was a gradient decrement trend from inlet to outlet. The closer it was to the inlet, the larger the wall load. The nearer it was to the outlet, the smaller the wall load. For the normal fluid-conveying pipeline, the wall load was evenly distributed with a grading gradient decrement trend. The pipeline in fouling condition showed a linear gradient decrement. Due to the roughness of the wall surface caused by stemming, the pressure direction changed with different surface conditions. Therefore, the wall load direction of the pipeline with stemming was scattered. Judging from the wall load, its maximum value constantly increased from 1.7×10^6 to 1.7×10^7 Pa, which indicated that the wall load increased with the severity of fouling. As shown in Figure 10, there was a clear difference between the fluid domain and the wall loads in normal pipeline and fouling pipeline. Hence, the fouling of the fluid-conveying pipeline was the main factor influencing the pipeline vibration. With the same inlet flow velocity as the premise, the more severe the pipeline fouling, the more violent the pipeline vibration.

D. Wall Displacement and Acceleration

By comparing the wall displacement shown in Figure 11 with the flow velocity of fluid domain shown in Figure 8, it is clear that the flow velocity increased where stemming was

heavily distributed, and the direction change became more obvious with increased wall displacement.

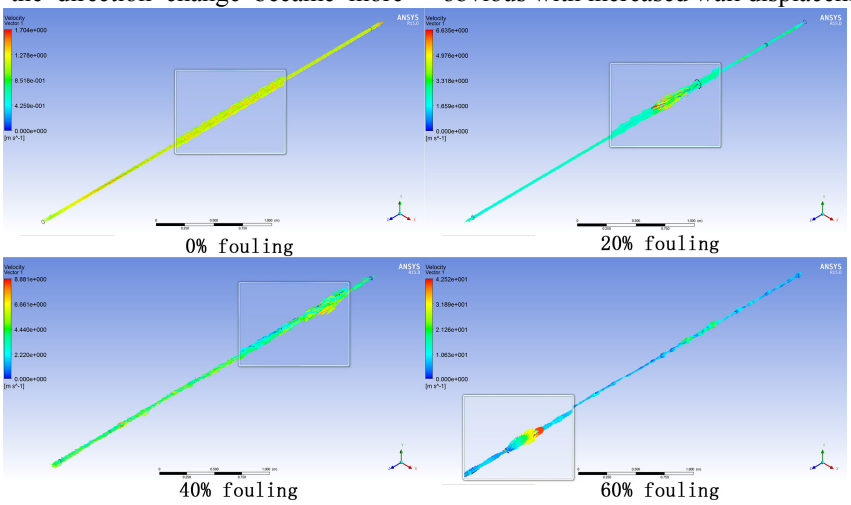

Figure 8. Flow velocity analysis of the fouling pipeline

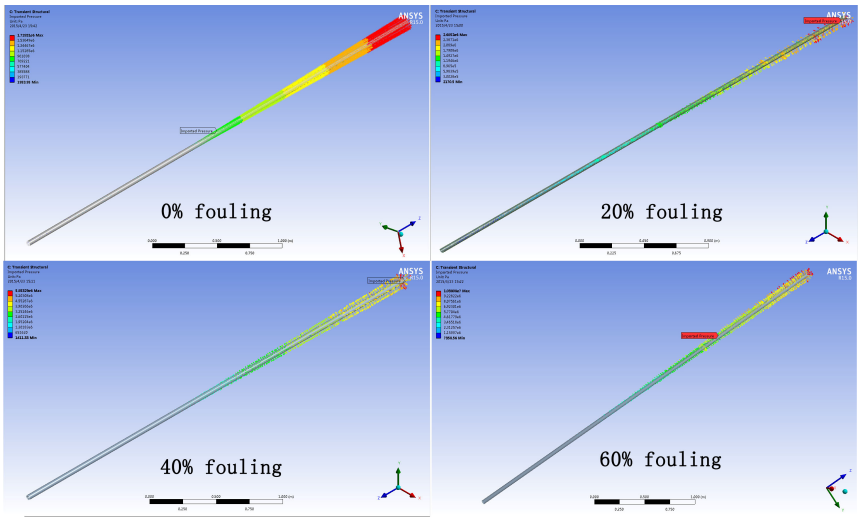

Figure 9. Wall load analysis of the fouling pipeline

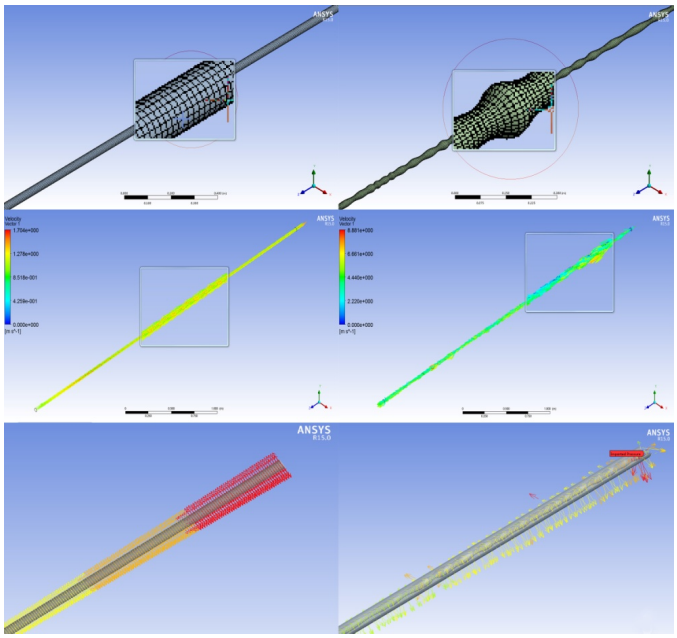

Figure 10. The contrast of the fluid domain and wall loads

Based on the average displacement value acquired in the steady condition of wall surface as shown in table III, it was discovered that the displacements were all different under the different flow velocity circumstances and different degrees of fouling. With the same inlet flow velocity, the pipeline displacement increased with the severity of fouling. While the displacement of pipeline with higher flow, velocity was higher in the same fouling condition, but otherwise gradually reduced. Therefore, with the premise of same inlet flow velocity, the displacement of pipeline in a steady condition was considered to be one of the parameters used to monitor and diagnose pipeline malfunction. However, in practical situations, an acceleration sensor was normally used to test the vibration of pipeline. It is of more practical significance to discuss the acceleration nephogram.

TABLE III DISPLACEMENTS CONTRAST OF DN20 PIPELINE (UNIT:m)

flow velocities	no fouling	20% fouling	40% fouling	60% fouling
0.4m/s	0.0066	0.0075	0.029	0.047
1.0m/s	0.0078	0.0087	0.038	0.051

The wall acceleration nephogram is shown in Figure 12. It was discovered that the distribution rule of acceleration was similar to displacement. In regions with heavily distributed stemming, the acceleration increased, and the flow direction changed more rapidly. As a consequence, the force on the pipeline wall increased as well, ultimately resulting in larger wall displacement and acceleration.

The acceleration in four fouling conditions and two different inlet flow velocities is summarized in Figure 13. In cases where 0% or 20% fouling exists, the variation of acceleration was insignificant regardless of whether the inlet flow velocity was 1.0 or 0.4 m/s. With 40% or 60% fouling, the acceleration changed substantially regardless of whether flow velocity was 1.0 or 0.4 m/s. The above results showed that only when the fouling was severe enough would it cause significant pipeline vibration. In the cases of 0%, 20%, and 40% fouling, the wall acceleration increased with the growth of flow velocity. However, with 60% fouling, the acceleration with a flow velocity of 0.4 m/s was similar to that of 1.0 m/s. Therefore, the inlet flow velocity and fouling severity were the main influencing factors in fluid-conveying pipeline vibration.

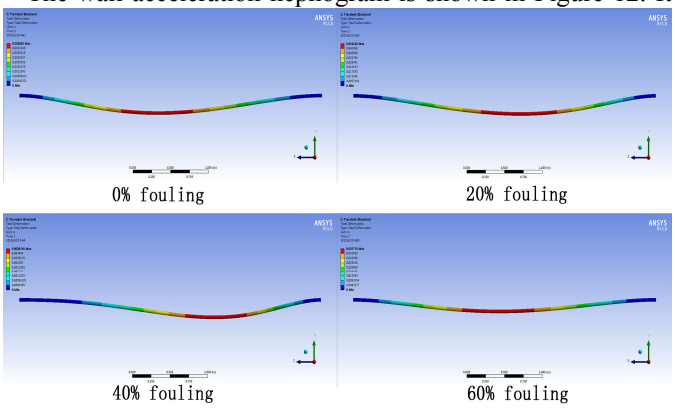

Figure 11. The displacement analysis of the fouling pipeline

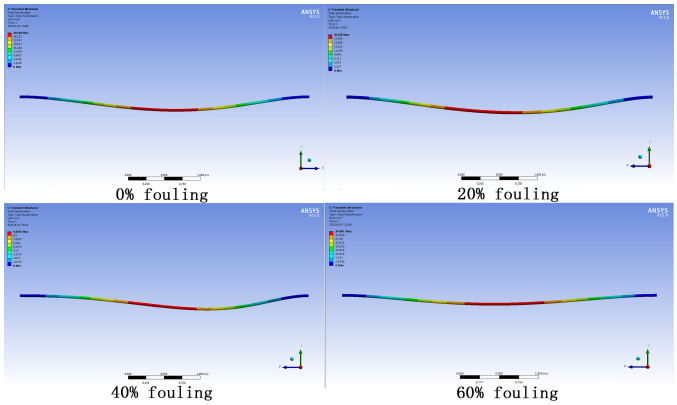

Figure 12. The acceleration analysis of the fouling pipeline

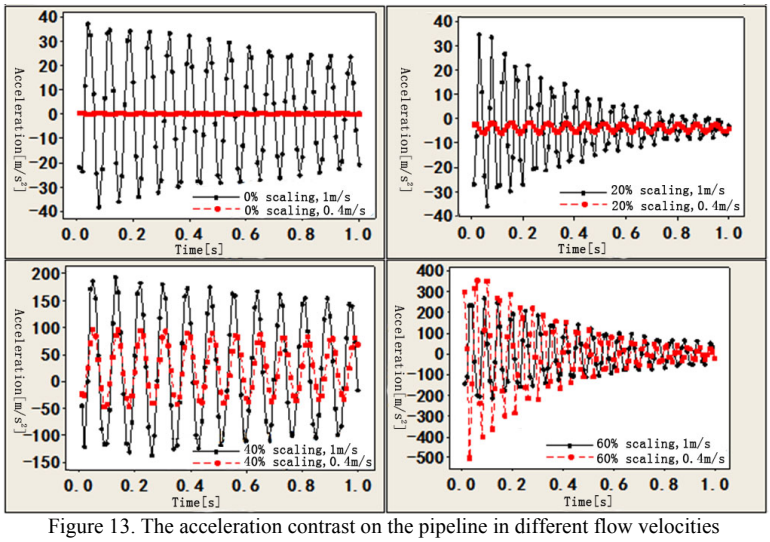

Figure 13. The acceleration contrast on the pipeline in different flow velocities

VII. EXPERIMENTS ON NORMAL PIPELINE

A. *Experiments*

In order to verify the feasibility and the correctness of using the ANSYS and CFX to establish the finite element model of fluid-conveying pipeline, this paper describes how experimental analysis was carried out on the experiment model under a single working condition. Using a fluid-conveying pipeline without fouling as a research subject, the experimental

facilities were as shown in Figure 14 and Figure 15. The facilities consisted of simple devices used to test the vibrations of pipeline with two pipe diameters under different flow velocity conditions. It included a wireless vibration signal test system, an experiment pool, pipeline located outside the pool, a stop valve at the front end of the pipeline, a pipeline pressure test instrument, flexible pipeline used to connect the pipeline and pool, a booster pump the at the pipeline inlet, and flow meters at both ends of the pipeline. The basic parameters of the experimental pipeline were as shown in Table IV. This paper conducted experiments respectively on the pipeline, using two different pipe diameters to simulate the vibrations caused by fluid with different inlet flow velocities. The pipeline inlet was connected to the pool and tap water pipeline. In addition, the pool was used to provide a water supply to the experimental pipeline through a water pump. The tap water increased the flow of pipeline to further expand the measuring range of the experiment. Flexible pipeline was used to connect the pump and pipeline to reduce the impact of the pump vibration on the whole experiment, since pump vibrations directly influence signal collection.

TABLE 4 THE BASIC PARAMETERS OF PIPELINES

Type	Material	Length	Pipeline diameter
DN20	galvanized pipe	2000mm	φ20×2mm
DN25	galvanized pipe	2000mm	φ25×2mm

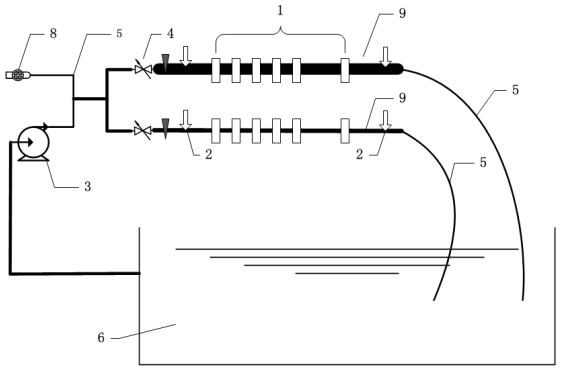

Figure 14. Schematic diagram of straight pipeline experiments:1-wireless vibration sensors, 2-flowmeters, 3-pumb, 4- water valve, 5- flexible pipeline, 6-pool, 7-press instrument, 8- tap water inlet, 9-pipelines.

Figure 15. Vibration test experiment of pipelines

The experiment primarily aimed to verify the consistency of the simulation and experimental model data of fluid-conveying pipeline. Hence, the acceleration data of vibration in the central portion of the pipeline was used for analysis—especially the acceleration value under different flow velocities at this position. Multiple high precision wireless sensors were installed at the center and at both ends of the pipeline through two fixed supports to collect vibration signals at the same time. Tap water was used for low flow to avoid the influences caused by pump vibration. Under circumstance where a demand for high flow velocity existed and the tap water alone failed to provide sufficient water, the pump was initiated and used to supply water. The flow velocity was set at 0.23, 0.33, 0.52, 0.74, and 1.01 m/s to respectively measure the acceleration of pipeline vibration under the influence of different flow velocities.

B. Data Comparison

TABLE V THE MAXIMUM ACCELERATIONS CONTRAST OF PIPELINES

Flow velocities (m/s)	DN20 simulation (g)	DN20 experiment (g)	DN25 simulation (g)	DN25 experiment (g)
0.23	0.0588	0.0736	0.0160	0.0546
0.33	0.0701	0.0848	0.0340	0.0615
0.52	0.1071	0.0864	0.0509	0.0610
0.74	0.2300	0.0728	0.0579	0.0933
1.01	0.3815	0.0905	0.0772	0.0601

Using the vibration data at the center of the DN20 pipeline as an example, Figure 16 shows that the data obtained by finite element analysis and experiment were generally similar with a velocity of 0.52 or 0.74 m/s. The acceleration data at a velocity of 0.33 m/s was within the same order of magnitude, while there was an order of magnitude difference at the velocity of 1.01 m/s. Meanwhile, the maximum vibration acceleration with different flow velocities was extracted. As shown in Table V, it can be seen that the maximum acceleration simulated by computer increased with the growth of inlet flow velocity with an extraordinarily clear linear growth trend. In addition, the experiment data also showed such a trend with a lower linear growth. When the inlet flow velocity was above 0.5 m/s, the maximum acceleration of the two models gradually deviated from each other. The data of the central portion of the DN25 pipeline showed basically the same trend. As shown in Figure 17, with inlet velocities of 0.52, 0.74, and 1.01 m/s, the main acceleration data were mostly the same. At a velocity of 0.33 m/s, the accelerations were within the same order of magnitude. Moreover, the maximum acceleration increased continuously with the growth of flow velocity.

By comparing several vibration acceleration experiments with the above five types flow velocities, it was discovered that the data simulated by computer and the experimental data were basically within the same order of magnitude range. Considering the influence of the water pump's vibration, instrumental error, boundary conditions of finite element analysis, and the differences in mesh quality, the results are

believed to be reasonable. In other words, it is acceptable to use ANSYS and CFX two-way coupling methods to simulate the fluid-conveying pipeline vibration to acquire the acceleration of the pipeline surface.

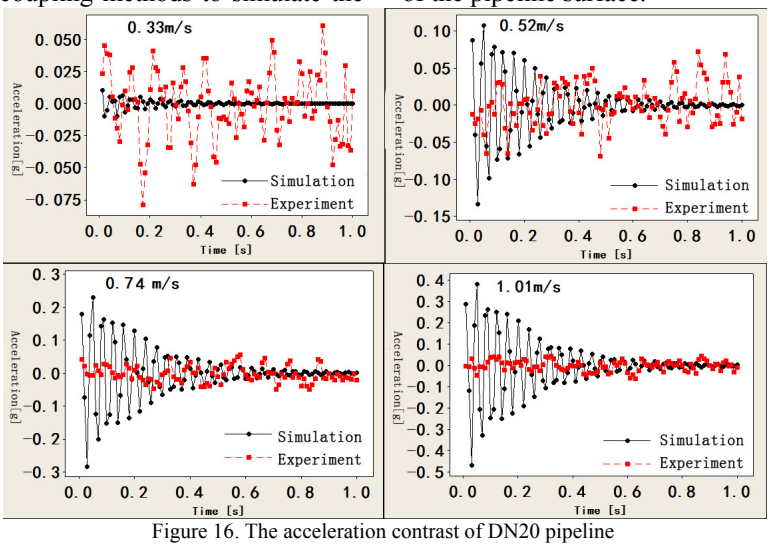

Figure 16. The acceleration contrast of DN20 pipeline

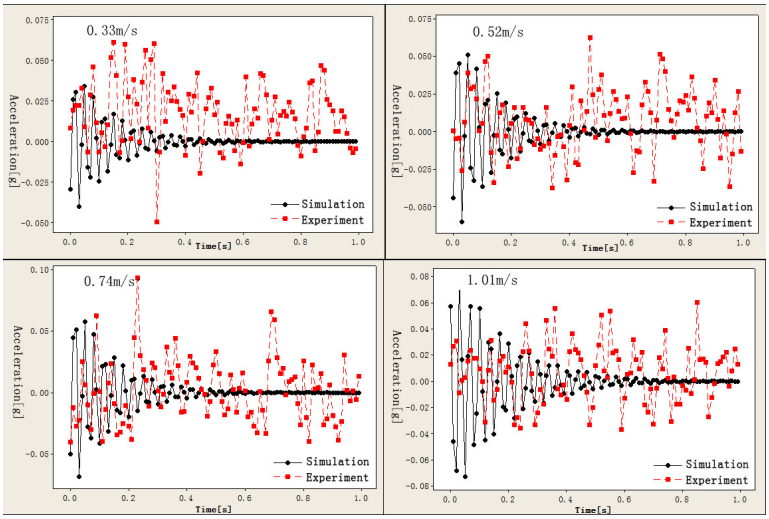

Figure 17. The acceleration contrast of DN25 pipeline

VIII. CONCLUSION

The pulsating flow triggered the pipeline vibration. After analyzing the forces of fluid-conveying pipeline both before and after fouling, it is believed that one of the causes of aggravated pipeline vibration is the increase of lateral force. ANSYS finite element analysis was used to establish the finite element model of fluid-conveying pipeline under the influence of fluid-solid coupling. Afterward, this paper conducted finite element analysis on the pipeline with different flow velocities and fouling levels. Furthermore, a group of pipeline vibration experiments were studied under the same normal condition. It found that the simulation data and the experimental data were basically in accordance.

The main conclusions were listed as follows:

1) By establishing the finite element model of fluid-conveying pipeline under normal conditions, this paper analyzed the flow velocity, direction, pipeline wall load, wall displacement and the acceleration of fluid domain in fluid-conveying pipeline of four cases. It was discovered that the wall load, wall displacement, and acceleration increased with the increase of inlet flow velocity. Therefore, the inlet flow velocity of fluid-conveying pipeline was one of influences over vibration.

2) By building the finite element model of fluid-conveying pipeline with different fouling levels, this paper conducted analysis on the flow velocity, direction, pipeline wall load, wall displacement, and acceleration of fluid domain in a fluid-conveying pipeline under the influence of four different levels of fouling (0%, 20%, 40%, and 60% fouling). It was discovered that the flow velocity and direction of fluid domain changed according to the variation of fouling positions. In addition, the wall load, wall displacement, and acceleration increased with increased degrees of fouling. Hence, the fluid-conveying pipeline fouling also had an impact on the pipeline vibration.

3) Two different experimental research studies were carried out on fluid-conveying pipeline, and with two different pipe diameters. This paper proved the correctness of the simulation model by comparing the simulation data with experiment data of non-fouling, fluid-conveying pipeline under the same working conditions.

REFERENCES

[1] A. Li, G. Xin, L. Zhou. "Research state on fluid-induced vibration of heat exchanger," (in Chinese), Liaoning Chemical Industry. 2007(12): 849-852.

[2] Y. Lai, M. Liu, Q. Dong. "Dynamic characteristic analysis of heat exchanger tube bundles with external fluid," (in Chinese), Pressure Vessel Technology. 2004(12): 22-25.

[3] A.K. Tiwari, P. Ghosh, J. Sarkar, H. Dahiya, and J. Parekh. "Numerical investigation of heat transfer and fluid flow in plate heat exchanger using nanofluids," International Journal of Thermal Sciences. 2014, 85(0): 93-103.

[4] W. Du, H. Wang, and L. Cheng. "Effects of shape and quantity of helical baffle on the shell-side heat transfer and flow performance of heat exchangers," Chinese Journal of Chemical Engineering. 2014, 22(3): 243-251.

[5] H. Bilirgen, S. Dunbar, EK. Levy. "Numerical modeling of finned heat exchangers," Applied Thermal Engineering. 2013, 61(2): 278-288.

[6] L. Cheng. "The flow induced vibration in heat exchanger," (in Chinese), China, Beijing: Science Press, 1995.

[7] JJD. Silva, AMN. Lima, FH. Neff, and JSD. Neto. "Fouling detection based on vibration analysis with the hammer impact test," Warsaw, Poland: Institute of Electrical and Electronics Engineers Inc., 2007.

[8] JJD. Silva, AMN. Lima, FH. Neff, and JSD. Neto. "Hammer impact test applied for fouling detection in pipelines," Sba Controle & Automao Sociedade Brasileira De Automatica. 2011, 22(6): 620-630.

[9] JJD. Silva, IB. Queiroz, AMN. Lima, and JSD. Neto. "Vibration analysis for fouling detection using hammer impact test and finite element simulation," Victoria, BC, Canada: Institute of Electrical and Electronics Engineers Inc., 2008.

[10] JJD. Silva, AMN. Lima, FH. Neff, and JSD. Neto. "Non-invasive fast detection of internal fouling layers in tubes and ducts by acoustic vibration analysis," Institute of Electrical and Electronics Engineers Inc., 2009.

[11] JJD. Silva, AMN. Lima, FH. Neff, and JSD. Neto. "Vibration analysis based on hammer impact test for multilayer fouling detection," Lisbon, Portugal: IMEKO-International Measurement Federation Secretariat, 2009.

[12] IGD. Carellan, P. Catton, C. Selcuk, and TH. Gan. "Methods for detection and cleaning of fouling in pipelines," Ioannina, Greece: Taylor and Francis Inc., 2012.

[13] J. Ren, L. Lin, S. Jiang. "Traveling wave method for pipe fluid-structure interaction," (in Chinese), Chinese Journal of Applied Mechanics. 2005(04): 530-535.

[14] B. Li, L. Xie, X. Guo, and Y. Wei. "Effect of flowing fluid on vibration frequencies of a thin-walled cylindrical tube," (in Chinese), Journal of Vibration and Shock. 2010(07): 193-195.

[15] Q. Guo, Q. Fan. "Simulation of Fluid-structure Interaction in Fluid Conveying Pipes by ANSYS," (in Chinese), Microcomputer Applications. 2010(04): 9-11.

[16] S. Li, B. Lei, Y. Li. "Modal analysis of pipe vibration under liquid-solid coupling condition," (in Chinese), China Metalforming Equipment & Manufacturing Technology. 2012(04): 76-78.

[17] Y. Wu, Y. Li, and Z. Liu. "the vibration analysis in full liquid pipe,"(in Chinese), Journal of Vibration, Measurement & Diagnosis. 2013(S2): 100-104.

[18] F. Wang, Z. Xu, W. Wu, and S. Liu. "Dynamic characteristic analysis of fluid-filled pipe under the action of fluctuating pressure," (in Chinese), Noise and Vibration Control. 2013(02): 11-14.

[19] Y. Wu, Y. Xu, F. "Wang. Blockage detection in water-supply pipelines based on auto-oscillation theory," (in Chinese), Journal of Harbin Institute of Technology. 2014(08): 45-50.

[20] J. Zhu. "Improvement of axial-coupled water hammer vibration equation," M.S. thesis, Kunming University of Science and Technology, Yunnan, China, 2014.

[21] B. Chen, M. Deng, J. Zhang, and Z. Yi. "Experimental study on parametric resonance of pipe conveying fluid based on laser vibration measurement technique," (in Chinese), Journal of Vibration, Measurement & Diagnosis. 2014(03): 560-564.

[22] H. Ji, N. Jiang, X. Huang. "Fluid-solid coupling analysis of fluid conveying pipes with finite element method," (in Chinese), Mechanical Engineer. 2016(01): 205-207.

[23] J. Huang, G. Chen, S. Lei, S. Wang and Z. Yu. "An experimental study of clogging fault diagnosis in heat exchangers based on vibration signals," IEEE Access, 2016(4): 1800-1809.

[24] W. Song, T. Xiao, J. Li. "On the present status and prospect of pipeline vibration control technology," (in Chinese), Journal of Safety and Environment. 2012(03): 184-188.

[25] J. Qian. "Study on noise and vibration reduction of providing water system to high building," (in Chinese), M.S. thesis, Tianjin University Of Science & technology, Tianjin, China, 2002.

[26] C. Yang. "Vibration characteristics of unsteady-fluid-filled pipe system and vibration restrain," (in Chinese), PHD thesis, Huazhong University of Science and Technology, Hubei, China, 2007.

[27] Y. Lai. "Analysis on dynamic characteristic and flow induced vibration of heat exchanger tube bundles," (in Chinese), PHD thesis, Nanjing Tech University, Jiangsu, China, 2006.

[28] V. Yakhot, SA. Orszag, S. Thangam, TB. Gatski, and CG. Speziale. "Development of turbulence models for shear flows by a double expansion technique," Physics of Fluids A (Fluid Dynamics). 1992, 4(7): 1510-1520.

JIANFENG HUANG(M'15) received the master's degree from the Guangdong University of Technology, Guangzhou, China, in 2006. He is currently pursuing the Ph.D. degree with the Institute of Safety Science Engineering, South China University of Technology, Guangzhou. Since 2006, he has been with the Guangdong University of Petrochemical Technology. He is currently an Associate Professor and the Department Head of Safety Engineering. Since 2013, he has been with the Guangdong Petrochemical Equipment Fault Diagnosis Key Laboratory. His research interests include industrial wireless sensor networks, petrochemical equipment fault diagnosis, and safety assessment.

GUOHUA CHEN received the Ph.D. degree in process safety from Nanjing Tech University, China. He is the Councilor of the China Occupational Safety and Health Association. He is currently a Professor and the Department Head of the Institute of Safety Science Engineering with the South China University of Technology, Guangzhou, China. His research interests include safety, reliability, and risk assessment technology about process equipment.

LEI SHU (SM'16) received the Ph.D. degree from the National University of Ireland, Galway, Ireland, in 2010. Until 2012, he was a Specially Assigned Researcher with the Department of Multimedia Engineering, Graduate School of Information Science and Technology, Osaka University, Japan. He is a member of the IEEE ComSoc, EAI, and ACM. Since 2012, he has been with the Guangdong University of Petrochemical Technology, China, as a Full Professor. He is the Founder of the Industrial Security and WSNs Laboratory. He is serving as the Editor-in-Chief of EAI Endorsed Transactions on Industrial Networks and Intelligent Systems, and an Associate Editor for a number of famous international journals. He served as more

than 50 various co-chairs for international conferences and workshops. His research interests include WSNs, multimedia communication, middleware, security, and fault diagnosis.

Yuanfang Chen (M'09) received her Ph.D. degree and M.S. degree from Dalian University of Technology, China. She currently works in Guangdong University of Petrochemical Technology as a Specially Assigned Researcher. She was an assistant researcher of Illinois Institute of Technology, U.S.A. with Prof. Xiang-Yang Li, from 2009 to 2010. She had been awarded the MASS 2009, 2013 IEEE Travel Grant, SIGCOMM 2013 Travel Grant, IWCMC 2009 and MSN 2010 Invited Paper. She has served as volunteer of MobiCom & MobiHoc 2010 and IEA-AIE 2012. She has been invited as the Session Chair of some good conferences, e.g., MobiQuitous 2013, ICA3PP 2015, and the TPC member, e.g., Globecom 2014, MobiApps 2014. She has served as reviewer of some top journals and conferences, e.g., IEEE TII, IEEE TPDS and Ad Hoc & Sensor Wireless Networks. She is an associate editor of EAI Endrosed Transactions on Industrial Networks and Intelligent Systems.

YU ZHANG received the Ph.D. degree from the Department of Civil Engineering, University of Nottingham, Nottingham, U.K., in 2011. She is currently a Senior Lecturer with the School of Engineering, University of Lincoln, Lincoln, U.K. Her research interests include intelligent systems and machine fault detection and diagnosis.